Hindawi
Journal of Mathematics
Volume 2023, Article ID 9618432, 12 pages
https://doi.org/10.1155/2023/9618432

Research Article

Reduced Gravity and Magnetohydrodynamic Effects on Transient Mixed Convection Flow Past a Magnetized Heated Cone Embedded in Porous Medium

Hossam A. Nabwey,[1,2] **Zia Ullah**,[3] **Asifa Ilyas**,[4] **Muhammad Ashraf**,[4] **Ahmed M. Rashad**,[5] **Sumayyah I. Alshber**,[1] **and Miad Abu Hawsah**[1]

[1]*Department of Mathematics, College of Science and Humanities, Prince Sattam Bin Abdulaziz University, Al-Kharj 11942, Saudi Arabia*
[2]*Department of Basic Engineering Science, Faculty of Engineering, Menoufia University, Shebin El-Kom 32511, Egypt*
[3]*Department of Mathematics and Statistics, The University of Lahore, Sargodha-Campus, Sargodha 40100, Pakistan*
[4]*Department of Mathematics, Faculty of Science, University of Sargodha, Sargodha 40100, Pakistan*
[5]*Department of Mathematics, Faculty of Science, Aswan University, Aswan 81528, Egypt*

Correspondence should be addressed to Hossam A. Nabwey; eng_hossam21@yahoo.com

Received 3 November 2022; Revised 24 December 2022; Accepted 19 April 2023; Published 4 May 2023

Academic Editor: Qingkai Zhao

The effects of reduced gravity on the periodic behavior of convective heat transfer characteristics of fluid flow along the magnetized heated cone embedded in porous medium is studied in the current contribution. The mathematical form of the nonlinear partial differential equations subject to the boundary conditions for the proposed unsteady model is presented. By employing appropriate dimensionless quantities, the mathematical equations are transformed into dimensionless form to get the numerical solutions of the proposed model. The dimensionless form is further condensed to a form that is more straightforward for smooth numerical computations. Later, large simulations are run using the implicit finite difference method for appropriate range of parameters values included in the flow model. The effect of reduced gravity parameter R_g, the Richardson parameter or mixed convection parameter λ, the Prandtl number Pr, and the porosity parameter Ω, on chief physical quantities, that is, velocity profile, temperature distribution, magnetic intensity, transient skin friction, transient rate of heat transfer, and transient current density are simulated and highlighted graphically. Additionally, via careful examination and intentional discussion of physical reasoning, the physical impacts of various factors on the material qualities are examined. Applications that motivate the present work is the reduced gravity effects due to which the other nongravity forces such as thermal volume expansion, density difference, and magnetic field can induce the fluid motion.

1. Introduction

The study of free/force convective heat transfer mechanism for reduced gravity in porous medium has inspired a significant number of research in the literature due to its wide range of practical applications. In this scenario, the flow phenomena is more complicated than in a pure thermal/solutal convection mechanism that combines the characteristics of conduction, diffusion, and advection to convey thermal energy from a warm climate to a cold one through a fluid. Researchers have paid a lot of attention to the analysis of single/multiphase flows as well as transfer processes in low gravity in the field of fluid dynamics. The main contribution in the reduced gravity has been based on the economic interests in order to optimize and better understanding of various processes. The material sciences, fluid dynamic, and combustion are three major research topics. Current commercial interests in the field of materials science include container less, processing, crystal growth, and metal/alloy/composite production. Under the influence of any

forceful flow, naturally occurring both convective heat rate transfer processes of gravity-independent diffusion, and gravity-driven advection usually combine to form a hotter mass of fluid. Due to thermal gradient diffusion, it loses density and rises as a result, absorbing heat and dispersing energy from the same mass.

The effect of fluctuations on heat transmission is very important topic in industry and engineering. In the molten/metal purification, macro/micro electronically devices, geophysics, and metallurgical systems, the impact of magnetohydrodynamic on fluctuating heat and magneto-fluid dynamics have received vital attentions. Many researchers have explored free or force convective heat rate mechanism on various nonmagnetic and magnetized shapes such as vertical heated plate, elliptic cylinders, plumes, and microporous channels using the aforementioned heat transfer ideas. To achieve numerical answers for specified boundary conditions, they employed a variety of techniques, including the series method, the Karman Pohlhausen simulation, the finite-element scheme, and the firing technique. It is possible to carry out experiments introduced gravity environments to a range of ground-based, flight-based, and space-based testing facilities. It has not yet been investigated how lowered gravity affects oscillatory convective flow along the electrical conductive cone embedded in a porous media. A physical model for the current physical phenomena has been developed using the concepts of oscillatory flow, heat transfer, magnetohydrodynamic, and reduced gravity.

Chun and Wuest [1] used the well-known light-cut approach to study how Marangoni convection in a floating zone changes from steady to oscillatory under the influence of decreasing gravity. Potter and Rily [2] explored free convection flow of a heated sphere at large Grashof number in the presence of reduced gravity. Anthony et al. [3] discussed the phenomena of heat transfer along the thermal bar by considering the temperature of maximum density for free convection boundary layer. Chamkha [4] focused on the impacts of heat generations on magnetohydrodynamic mixed convective flow from a rotating cone immersed in porous material. The effects of thermal dispersion on mixed heat mass transfer by convective flow on vertical form plate imbedded in porous media were explored by Chamkha and Khaled [5]. The effects of radiative mixed convective simulation of optically dense viscous fluid next to the isothermal cone immersed in porous material were numerically treated by Yih [6]. The researcher in [7] investigated the impact of heatmass rate on the free convection flow of visco elastic electrical conductive fluid along the vertical porous heated plate numerically.

Dessie and Kishan's stretching sheet experiment [8] that was immersed in porous material was investigated by the magnetohydrodynamic convective boundary analysis. With regard to the nonfluctuating stagnated-point heat rate properties of visco elastic fluid through vertical stretched shape immersed in porous material, the researcher [9] investigated the impacts of thermal radiation. In the presence of viscous dissipation and a nonuniform heat source, investigations in [10] of magnetic free/force convective analysis of fluid flow through stretched sheet contained in porous material. Malik et al. [11] have shown the impact of thermal conductivity and temperature dependent viscosity on the turbulent incompressible flow and heat transfer dynamics of a viscous fluid on a revolving vertical cone. The vertical heated cone encased in porous material was considered to a constant, electrical free/force convective boundary-layer flow by Sudhagar et al. [12]. Raju et al. [13] looked at the mechanism of heat rate on an unstable convective Casson circular fluid problem on rotational vertical heated-cone immersed in porous material. The effect of reduced gravity on free convective heat transfer from a finite, flat, and vertical heated plate was numerically studied by Lotto et al. [14]. The effect of viscous dissipation on fluctuating momentum and transient thermal boundary layer free/force convective flow over a sphere was deduced in [15]. Ashraf and Fatima [16] have investigated the influence of fluctuating shear stress and heat rate of oscillatory convective flow around various points of heated sphere in the influence of dissipations by numerical simulation. The study of the associated process of mixed convection flow and thermophoretic transportation around the surface of the sphere was the main objective of Alhamid's et al. work [17]. The heat rate simulations of improved thermal hydraulic phenomena in three dimension circular pipe with various structure configuration parameters has investigated by the researchers [18–21]. The effects of MHD and lowered gravity on periodic free/force convective and electrical conductive fluid across a thermal and nonconducting horizontal circular cylinder has discussed in [18]. Rasool et al. [22] numerically examined EMHD nanofluid flows across a Riga pattern that is positioned horizontally in a Darcy-Forchheimer porous medium. Rauf et al. [23] explored the mechanism of heat transfer and MHD micro polar ferro fluid flow above a nonlinearly stretching sheet. Oreyeni et al. [24] proposed the model of the importance of changing thermophysical characteristics and exponential space-based heat generation on the dynamics of the Casson fluid across a stratified surface with nonuniform thickness. Shah et al. [25] focused on unsteady nonlinear nanofluid convection flow in an infinite rectangular channel. Analytical research is conducted on the generalized fractional thermal transport-induced unsteady natural convection flow of viscous fluids in a circular cylinder by Vieru et al. [26]. Babu et al. [27] predicted the problem of a permeable exponentially stretchable plate surface with a two-dimensional MHD micropolar fluid with heat and mass transport transients. The suggested model modifies the solute and energy equations to account for the effects of activation energy and Brownian motion. Zeeshan et al. [28] examined a numerical insight of activation energy in transient micropolar nanofluid flow formed by an exponentially extended plat surface with thermal radiation effects. Abderrahmane et al. [29] developed a numerical problem of 3D triangular porous cavity with zigzag walls and a rotating cylinder, MHD hybrid nanofluid mixed convection heat transfer and entropy generation. Santhosh et al. [30] analyzed the effects of optically dense and chemically reactive Casson fluid above a cone, plate, and wedge with gyrotactic microorganisms subjected to the Cattaneo–Christov heat flux model.

Nagendramma et al. [31] presented the dynamic flow of an incompressible triple diffusive fluid through a linearly stretched surface. Shahzad et al. [32] created a model to describe the properties of the bio-convection and moving microorganisms in the flows of a magnetized generalized Burgers' nanofluid with Fourier's and Fick's laws in a stretched sheet. Ram et al. [33] focused on a nonlinear mathematical model of a liquid moving to a micropolar stagnation point along a stretchable permeable device while variable reactive species and heat sink/source impacts are present. Salawu et al. [34] discussed the flow rate, temperature distribution, and entropy formation of the magnetized hybrid Prandtl-Eyring nanofluid along the inside parabolic solar trough collector of an aircraft wing. Salawu et al. [35] examined double exothermic reaction–diffusion of thermal ignition branched chain and couple stress fluid with exponential Reynold's viscosity and optical radiation. A theoretical analysis of the coupled thermo-solutal free convection flow of a magnetized fluid from an exponentially stretched magnetic sensor (Riga plate) surface in two dimensions is presented by Shamshuddin et al. [36].

According to the aforementioned literature review, transient mixed convective flow along the magnetized heated cone embedded in porous medium with the inclusion of reduced gravity in the reduced form of Navier Stokes equation has not yet been studied. Using concepts from the prior literature review and the works of Chun and Wuest [1], Anthony et al. [3], Ashraf et al. [15], and Al-Obaidi and Alhamid [18], the transient and fluctuating mixed convective flow mechanism along an electrically conducted cone embedded in porous medium with effects of weak gravity is developed. The transient heat transfer, skin friction, and current density quantities are computed after first examining the fluid velocity, magnetic field, and temperature profiles from the steady part of the proposed model.

2. Flow Problem and Mathematical Description

Consider the two-dimensional oscillating mixed convective boundary layer fluid flow phenomena over the surface of a magnetized heated cone immersed in porous material. The magnetized flow geometry is plotted in Figure 1 where y is considered normal to the cone's surface and x is considered along the magnetized surface. u and v, respectively, stand for the x- and y-directional velocity components. B_x stands for the component of the magnetic field at the cone's surface, B_y for the taking of the surface normal, and $U(x,t)$ for the cone's external fluid velocity. Additionally, the magnetic field intensity is identical at the magnetized cone's surface. The boundary layer equations' by following [21] and by including the idea of magnetized cone the dimensionless form shows the flow behavior.

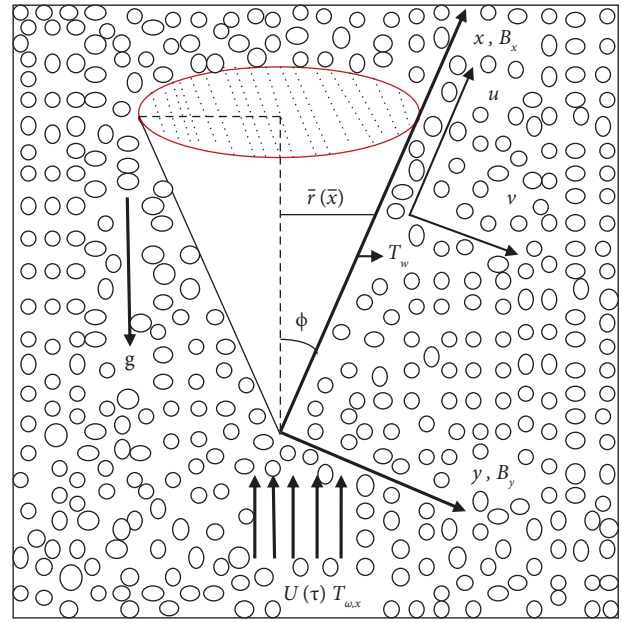

Figure 1: Magnetized heated cone and coordinate system.

The relationship between density and temperature is as follows when the temperature is sufficiently close to T_m:

$$\frac{\rho-\rho_m}{\rho_m} = -\gamma(T-T_m)^2, T \longrightarrow T_m \pm \Delta\text{Tasy} \longrightarrow \pm\infty, \tag{1}$$

for a certain fixed ΔT. Consider region $y \geq 0$ subject to the boundary constraints in order to obtain the symmetry in this case. By following [3], here, $T_\infty = T_m + \Delta T$ is related to by equation (1) and has the formula $T_\infty = T_m + \Delta T$. The reduced gravity can be easily defined as $g' = g(\rho - \rho_\infty/\rho_\infty)$ (i.e., the fluid particles of acceleration with density ρ_m). Equation (1), then becomes as follows:

$$g' = g\gamma\frac{\rho_m}{\rho_\infty}(T_\infty - T_m)^2. \tag{2}$$

Following [2, 27, 37], the dimensionless form of the boundary conditions and the governing continuity, momentum, magnetic, and energy equations in the presence of reduced gravity is defined as follows:

$$\frac{\partial\overline{u}}{\partial\overline{x}} + \frac{\partial\overline{v}}{\partial\overline{y}} = 0, \tag{3}$$

$$\frac{\partial\overline{b}_x}{\partial\overline{x}} + \frac{\partial\overline{b}_y}{\partial\overline{y}} = 0, \tag{4}$$

$$\frac{\partial \overline{u}}{\partial \tau} + \overline{u}\frac{\partial \overline{u}}{\partial \overline{x}} + \overline{v}\frac{\partial \overline{u}}{\partial \overline{y}} = \frac{\partial^2 \overline{u}}{\partial \overline{y}^2} + \xi\left(\overline{b}_x\frac{\partial \overline{\mathrm{b}}_{\mathrm{x}}}{\partial \overline{y}} + \overline{b}_y\frac{\partial \overline{\mathrm{b}}_{\mathrm{x}}}{\partial \overline{y}}\right) - \Omega(\overline{u}) + \lambda R_{\mathrm{g}}\left(2\overline{\theta} - \overline{\theta}^2\right), \tag{5}$$

$$\frac{\partial \overline{\mathrm{b}}_x}{\partial \tau} + \overline{u}\frac{\partial \overline{\mathrm{b}}_x}{\partial \overline{x}} + \overline{v}\frac{\partial \overline{\mathrm{b}}_x}{\partial \overline{y}} - \overline{b}_x\frac{\partial \overline{\mathrm{u}}}{\partial \overline{x}} - \overline{b}_y\frac{\partial \overline{\mathrm{u}}}{\partial \overline{y}} = \frac{1}{\gamma}\frac{\partial^2 \overline{\mathrm{b}}_x}{\partial \overline{y}^2}, \tag{6}$$

$$\frac{\partial \overline{\theta}}{\partial \tau} + \overline{u}\frac{\partial \overline{\theta}}{\partial \overline{x}} + \overline{v}\frac{\partial \overline{\theta}}{\partial \overline{y}} = \frac{1}{P_r}\frac{\partial^2 \overline{\theta}}{\partial \overline{y}^2}. \tag{7}$$

The dimensionlized boundary conditions are as follows:

$$\begin{aligned} &\overline{u} = \overline{v} = 0, \overline{b}_y = 0, \overline{b}_x = 1, \overline{\theta} = 1\ at \quad \overline{y} = 0 \\ &\overline{u} \longrightarrow \overline{U}(\tau), \overline{\theta} \longrightarrow 0, \overline{\mathrm{b}}_x \longrightarrow 0\ as\ \overline{y} \longrightarrow \infty. \end{aligned} \tag{8}$$

In the above equations (3)–(7), using proposed boundary conditions (8), Richardson parameter λ and γ represent the porosity number Ω, B_0 is the exact strength of the magnetic field at the surface, Pr stands for Prandtl parameter, and R_{g} is the reduced gravity number.

$$\begin{aligned} &\xi = \frac{\mu {B_0}^2}{\rho {U_\infty}^2}, \alpha = \frac{\kappa}{\rho C_p}, \lambda = \frac{G_{r_L}}{{Re_L}^2}, Re_L = \frac{U_\infty L}{\nu}, D_{al} = \frac{k}{\epsilon^+ L^2}, \theta = \frac{T - T_\infty}{T_m - T_\infty} \\ &P_r = \frac{\nu}{\alpha}, G_{r_L} = \frac{g\beta\Delta T L^3}{\nu^2}\cos\alpha, \gamma = \frac{\nu}{\nu_m}, \Omega = \frac{1}{D_{al.Re_L}}, R_{\mathrm{g}} = \frac{\mathrm{g}^{'}}{g\beta\Delta T}, \end{aligned} \tag{9}$$

where is the oscillation's amplitude ε and $|\varepsilon| \ll 1$ is assumed, the frequency parameter ω takes the form $U(\tau) = 1 + \epsilon e^{i\omega\tau}$. The velocity u, v, magnetic field b_x, b_y and temperature distribution θ is expressed in form of fluctuating and nonfluctuating.

$$\begin{aligned} &\overline{u} = u_s + \epsilon u_t e^{i\omega\tau}, \overline{v} = v_s + \epsilon v_t e^{i\omega\tau}, \overline{\mathrm{b}}_x = \mathrm{b}_{xs} + \epsilon \mathrm{b}_{xt} e^{i\omega\tau} \\ &\overline{b}_y = \mathrm{B}_{ys} + \epsilon \mathrm{b}_{yt} e^{i\omega\tau}, \overline{\theta} = \theta_{\mathrm{s}} + \epsilon\theta_{\mathrm{t}} e^{i\omega\tau}. \end{aligned} \tag{10}$$

We can independently substitute the dimensionless fluctuating and nonfluctuating equations by equating-like powers of $O(\varepsilon^0)$ and $O(\varepsilon e^{i\omega\tau})$, using equation (10), and by doing the following [15, 16]:

2.1. For Steady Components.

$$\frac{\partial u_s}{\partial x} + \frac{\partial v_s}{\partial y} = 0, \tag{11}$$

$$u_s\frac{\partial u_s}{\partial x} + v_s\frac{\partial u_s}{\partial y} = \frac{\partial^2 u_s}{\partial y^2} + \xi\left(b_{xs}\frac{\partial b_{xs}}{\partial x} + b_{ys}\frac{\partial b_{xs}}{\partial y}\right) - \Omega u_s + \lambda R_{\mathrm{g}}\left(2\theta_s - {\theta_s}^2\right), \tag{12}$$

$$\frac{\partial b_{xs}}{\partial x} + \frac{\partial b_{ys}}{\partial y} = 0, \tag{13}$$

$$u_s\frac{\partial b_{xs}}{\partial x} + v_s\frac{\partial b_{xs}}{\partial y} - b_{xs}\frac{\partial u_s}{\partial x} - b_{ys}\frac{\partial u_s}{\partial y} = \frac{1}{\gamma}\frac{\partial^2 b_{xs}}{\partial y^2}, \tag{14}$$

$$u_s\frac{\partial \theta_s}{\partial x} + v_s\frac{\partial \theta_s}{\partial y} = \frac{1}{P_r}\frac{\partial^2 \theta_s}{\partial y^2}. \tag{15}$$

With appropriate boundary conditions:

$$u_s = v_s = 0, b_{ys} = 0, b_{xs} = 1, \theta_s = 1 \text{ at } y = 0$$
$$u_s \longrightarrow 1, \theta_s \longrightarrow 0, b_{xs} \longrightarrow 0 \text{ as } y \longrightarrow \infty. \tag{16}$$

By employing the Stokes conditions of fluctuations given in equation (17), the separable real and the separable imaginary equations can be obtained by referring to [15] as follows:

$$u_t = u_1 + iu_2, v_t = v_1 + iv_2, \theta_t = \theta_1 + i\theta_2, b_{xt} = b_{x1} + ib_{x2}, b_{yt} = b_{y1} + ib_{y2}. \tag{17}$$

2.2. For Real Components.

$$\frac{\partial u_1}{\partial x} + \frac{\partial v_1}{\partial y} = 0, \tag{18}$$

$$-\omega u_2 + u_s\frac{\partial u_1}{\partial x} + u_1\frac{\partial u_s}{\partial x} + v_s\frac{\partial u_1}{\partial y} + v_1\frac{\partial u_s}{\partial y} = \frac{\partial^2 u_1}{\partial y^2} + \xi\left(b_{xs}\frac{\partial b_{x1}}{\partial x} + b_{x1}\frac{\partial b_{xs}}{\partial x} + b_{ys}\frac{\partial b_{x1}}{\partial y} + b_{y1}\frac{\partial b_{xs}}{\partial y}\right) - \Omega u_1 + 2\lambda R_g(\theta_1 - \theta_1\theta_s), \tag{19}$$

$$\frac{\partial b_{x1}}{\partial x} + \frac{\partial b_{y1}}{\partial y} = 0, \tag{20}$$

$$-\omega b_{x2} + u_s\frac{\partial b_{x1}}{\partial x} + u_1\frac{\partial b_{xs}}{\partial x} + v_s\frac{\partial b_{x1}}{\partial y} + v_1\frac{\partial b_{xs}}{\partial y} - b_{xs}\frac{\partial u_1}{\partial x} - b_{x1}\frac{\partial u_s}{\partial x} - b_{ys}\frac{\partial u_1}{\partial y} - b_{y1}\frac{\partial u_s}{\partial y} = \frac{1}{\gamma}\frac{\partial^2 b_{x1}}{\partial y^2}, \tag{21}$$

$$-\omega\theta_2 + u_s\frac{\partial \theta_1}{\partial x} + u_1\frac{\partial \theta_s}{\partial x} + v_s\frac{\partial \theta_1}{\partial y} + v_1\frac{\partial \theta_s}{\partial y} = \frac{1}{P_r}\frac{\partial^2 \theta_1}{\partial y^2}, \tag{22}$$

along with boundary conditions:

$$u_1 = v_1 = 0, b_{y1} = 0, b_{x1} = 1, \theta_1 = 0 \text{ at } y = 0$$
$$u_1 \longrightarrow 1, \theta_1 \longrightarrow 0, b_{x1} \longrightarrow 0 \text{ as } y \longrightarrow \infty. \tag{23}$$

2.3. For Imaginary Components.

$$\frac{\partial u_2}{\partial x} + \frac{\partial v_2}{\partial y} = 0, \tag{24}$$

$$\omega u_1 + u_s\frac{\partial u_2}{\partial x} + u_2\frac{\partial u_s}{\partial x} + v_s\frac{\partial u_2}{\partial y} + v_2\frac{\partial u_s}{\partial y} = \frac{\partial^2 u_2}{\partial y^2} + \xi\left(b\frac{\partial b_{x2}}{\partial x} + b_{x2}\frac{\partial b_{xs}}{\partial x} + b_{ys}\frac{\partial b_{x2}}{\partial y} + b_{y2}\frac{\partial b_{xs}}{\partial y}\right) - \Omega u_2 + 2\lambda R_g(\theta_2 - \theta_2\theta_s), \tag{25}$$

$$\frac{\partial b_{x2}}{\partial x} + \frac{\partial b_{y2}}{\partial y} = 0,$$
$$\omega b_{x1} + u_s\frac{\partial b_{x2}}{\partial x} + u_2\frac{\partial b_{xs}}{\partial x} + v_s\frac{\partial b_{x2}}{\partial y} + v_2\frac{\partial b_{xs}}{\partial y} - b_{xs}\frac{\partial u_2}{\partial x} - b_{x2}\frac{\partial u_s}{\partial x} - b_{ys}\frac{\partial u_2}{\partial y} - b_{y2}\frac{\partial u_s}{\partial y} = \frac{1}{\gamma}\frac{\partial^2 b_{x2}}{\partial y^2}, \tag{26}$$

$$\omega\theta_1 + u_s\frac{\partial\theta_2}{\partial x} + u_2\frac{\partial\theta_s}{\partial x} + v_s\frac{\partial\theta_2}{\partial y} + v_2\frac{\partial\theta_s}{\partial y} = \frac{1}{P_r}\frac{\partial^2\theta_2}{\partial y^2}, \tag{27}$$

along with boundary conditions:

$$\begin{aligned} u_2 = v_2 = 0, b_{y2} = 0, b_{x2} = 0, \theta_2 = 0 \text{ at } y = 0 \\ u_2 \longrightarrow 0, \theta_2 \longrightarrow 0, b_{x2} \longrightarrow 0 \text{ as } y \longrightarrow \infty. \end{aligned} \tag{28}$$

3. Solution Methodology and Computational Procedure

The governing dimensionless nonfluctuating and fluctuating models are computed by the very effective and accurately tested finite difference simulation. This transformation discretizes the dimensionlized controlling imaginary, real, and stable equations that were previously derived. Due to this, the steady position of each independent and dependent quantities is converted into an acceptable form by using [2, 16, 18, 19]. The FDM approach is once more used to solve the aforementioned primitive generated equations (11)–(28). The converted algebraic primitive equations with U, V, θ, and φ unknown quantities can be quantitatively demonstrated by applying the Gaussian elimination technique in the form of a tridiagonal matrix. Equation (29), where A_s, A_t, and A_m are amplitudes and α_s, α_t, and α_m are phase angles as given in [19, 20], addresses the outcomes from periodic transient shear stress τ_s, current density τ_m, and heat transfer τ_t along the magnetized heated cone.

$$\begin{aligned} \tau_s &= \left(\frac{\partial U}{\partial Y}\right)_{y=0} + \varepsilon\left|A_s\right|\mathrm{Cos}\left(\omega t + \alpha_s\right), \\ \tau_t &= \left(\frac{\partial \theta}{\partial Y}\right)_{y=0} + \varepsilon\left|A_t\right|\mathrm{Cos}\left(\omega t + \alpha_t\right), \\ \tau_m &= \left(\frac{\partial \varphi}{\partial Y}\right)_{y=0} + \varepsilon\left|A_m\right|\mathrm{Cos}\left(\omega t + \alpha_m\right), \end{aligned} \tag{29}$$

where

$$\begin{aligned} A_s = \left(u_1^{\,2} + u_2^{\,2}\right)^{(/)}, A_t = \left(\theta_1^{\,2} + \theta_2^{\,2}\right)^{(/)}, A_m = \left(\varphi_{x1}^{\,2} + \varphi_{x2}^{\,2}\right)^{(/)} \\ \alpha_s = \tan^{-1}\left(\frac{u_2}{u_1}\right), \alpha_t = \tan^{-1}\left(\frac{\theta_2}{\theta_1}\right), \alpha_m = \tan^{-1}\left(\frac{\varphi_{x2}}{\varphi_{x1}}\right) \end{aligned} \tag{30}$$

4. Results and Discussions

In the present study, mixed convection periodic flow along a magnetized heated cone embedded in a porous material under the influence of reduced gravity effects has numerically simulated. For coupled form of the partial differential equations subjected to the boundary conditions, the proposed unsteady nonlinear mathematical model is presented graphically. The primitive variable formulation is used to transform the system of partial differential equations into primitive form for smooth integration and to design the numerical algorithm. Later, large simulations are run using the implicit finite difference method for a range of parameter values. The reduced gravity parameter R_g, the Richardson parameter λ, the Prandtl number Pr, the porosity parameter Ω, and several other fixed parameters were all used to reach the numerical solutions of the coupled dimensionlized equations. Plots are sketched for several governing parameters in the necessary modeled equations, including magnetic intensity, temperature and velocity profile, transient shear tress graph, graph of heat rate, and graph of current density. The numerical and graphical outcomes are drafted for various developing parameters with favorable choices.

The physical behavior of the magnetic ϕ and temperature θ field plots and velocity distribution for various choices of the reduced gravity parameter R_g are shown in Figures 2(a)–2(c). In graphs, the significant differences in the velocity plot U, magnetic ϕ, and temperature θ field plots were shown for each value of R_g. The prominent quantity of the velocity U plot is found at $R_g = 1.5$ and at $R_g = 0.1$ for the magnetic ϕ and temperature θ plots, respectively. Although fluid's motion may be produced by number of causes, such as surface-tensions and the density fluctuations, in the absence of a gravitational field, buoyant energies can induce the motion of fluid in the lower gravity within weak gravitational-fields. By asymptotically satisfying the specified boundary criteria, the graphical outputs are designed with noticeable differences. The physical effects of the porosity parameter Ω are shown by the graphical representations of the aforementioned unidentified physical variables in Figures 3(a)–3(c). Plots make it clear that while velocity value profiles are descending for decreasing values of Ω, magnetic plot and temperature plots are ascending. It is emphasized that lower results in magnetic plot and temperature plots are deduced with the highest Ω choices. This is because as intermolecular connections decline, the fluid's thermal conductivity also declines. Each plot presents good variations for each value of Ω with prominent asymptotic behavior. Figures 4(a)–4(c) are showing simulations for ϕ, θ, and u for various choices of Richardson parameter λ. The graphs demonstrate that u is increased with increasing λ values while ϕ and θ are decreased in the presence of Pr = 7.0. According to a physical point of view, this can be evident that when Pr is increased, heat transmission with respect to thermal-diffusion is reduced, and the thickness of the fluid's velocity falls due to the retarding force the fluid must contend with while moving. It is pertinent to mention that the amplitude of transient skin friction is increased for increasing values of mixed convection parameter. The increasing behavior of mixed convection parameter acts like pressure gradient R_i.

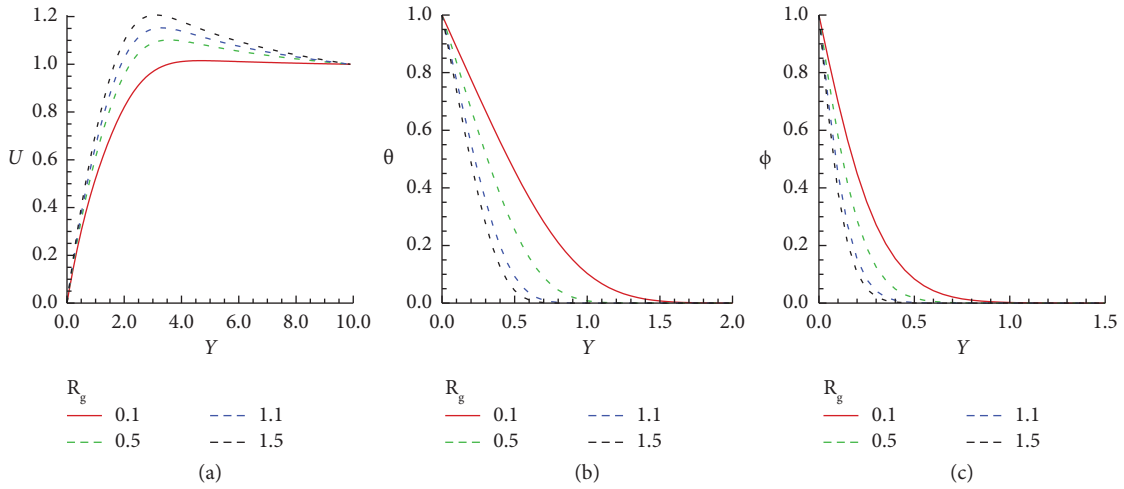

Figure 2: (a)–(c) Nonoscillating/steady plots of U, θ, ϕ, against R_g.

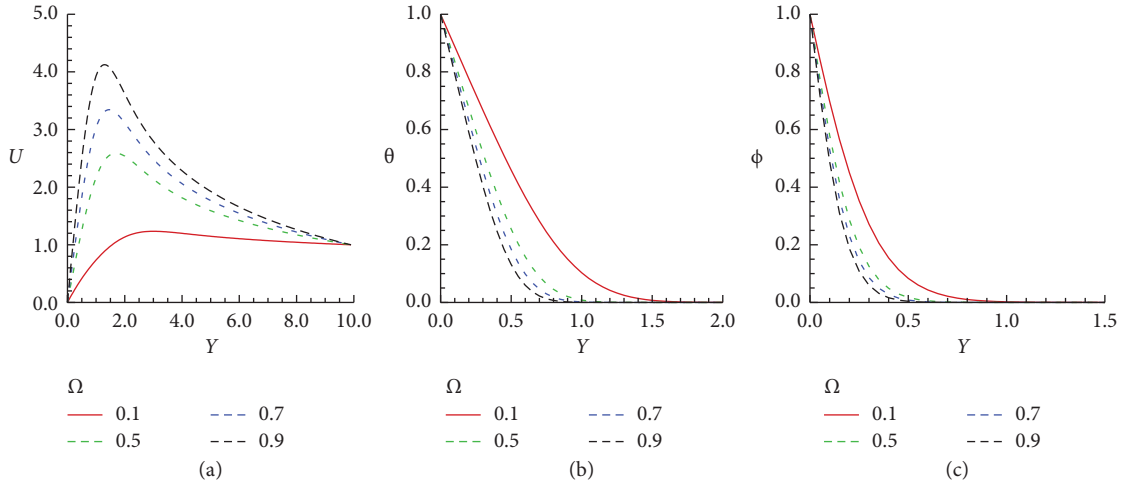

Figure 3: (a)–(c) Nonoscillating/steady plots of U, θ, ϕ, against Ω.

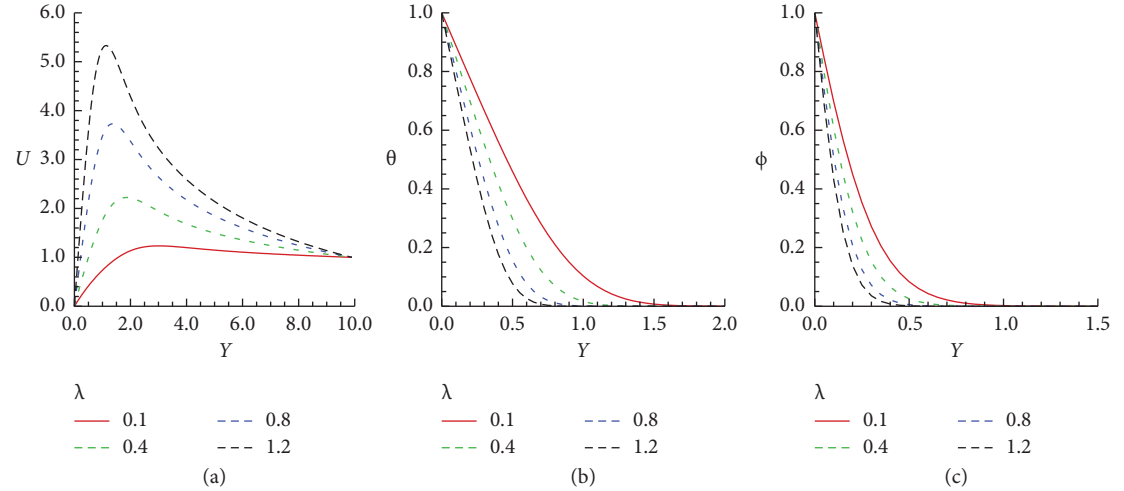

Figure 4: (a)–(c) Nonoscillating/steady plots of U, θ, ϕ, against λ.

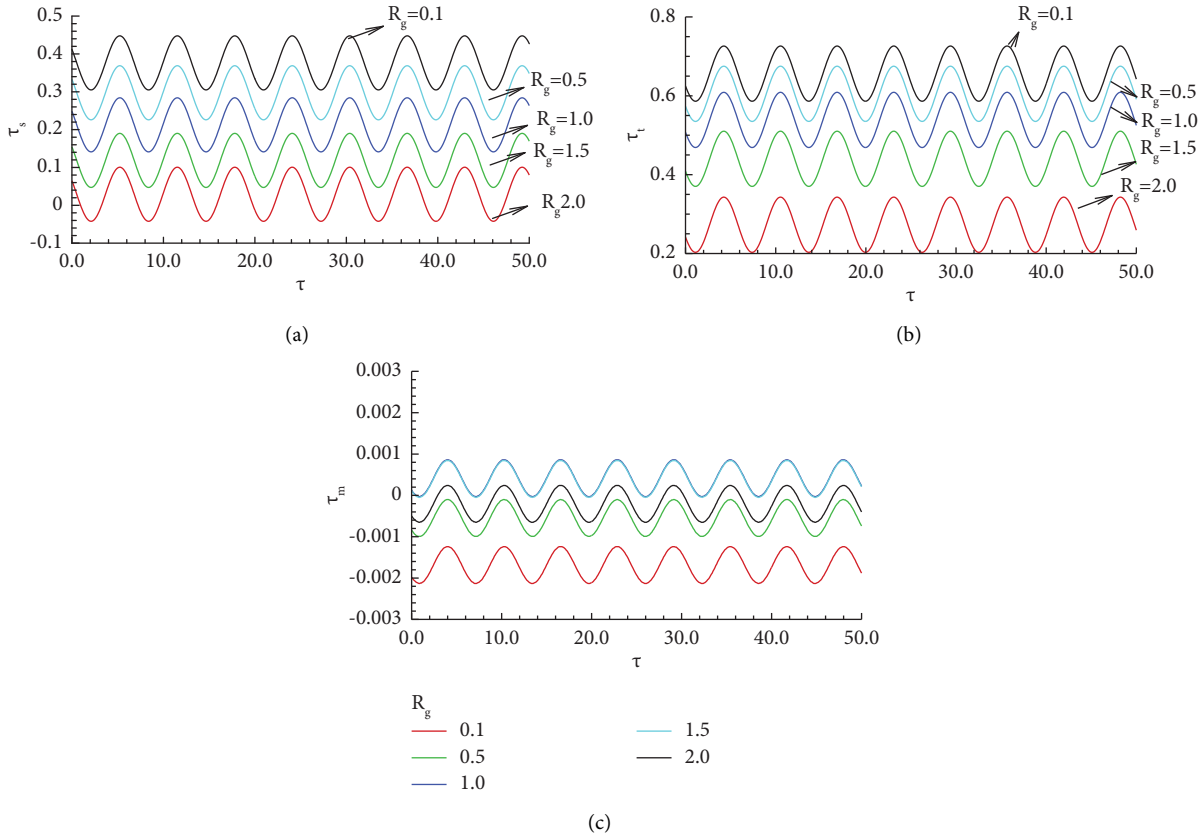

Figure 5: (a)–(c) The oscillating plots of τ_s, τ_m, τ_t, against R_g.

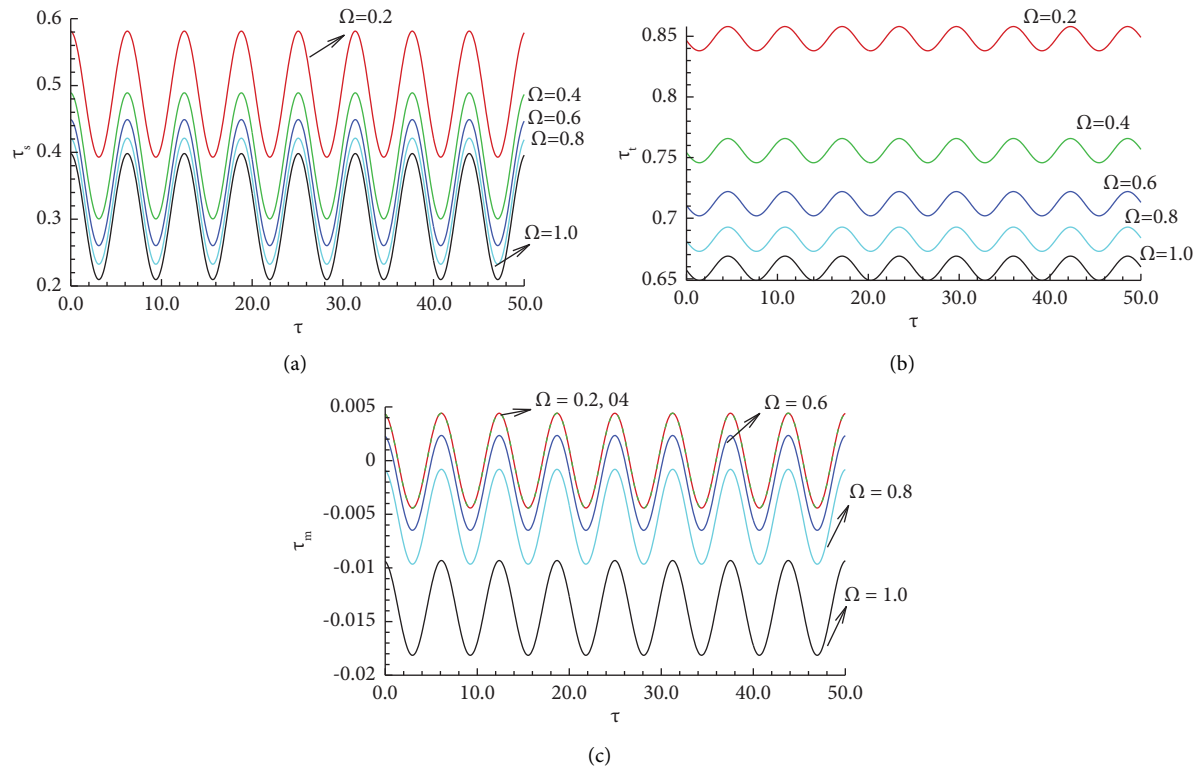

Figure 6: (a)–(c) The oscillating plots of τ_s, τ_m, τ_t, against Ω.

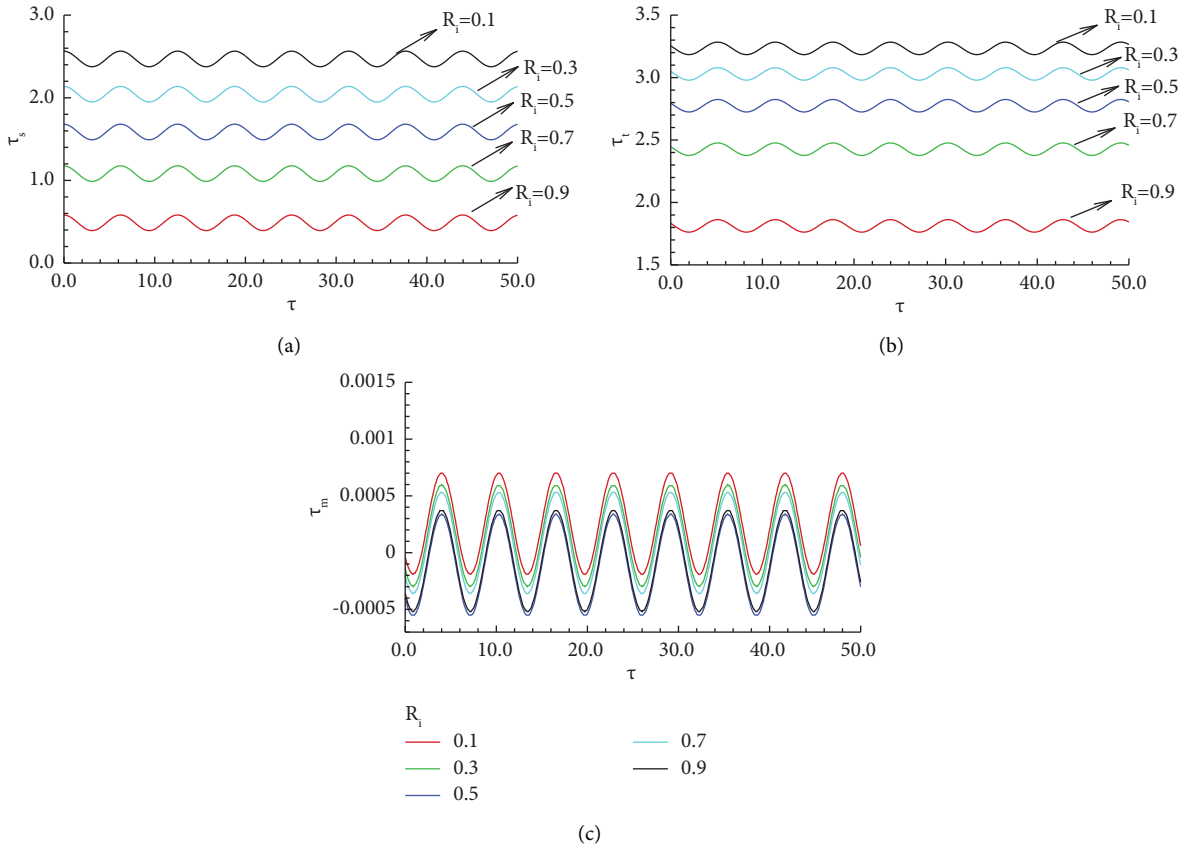

Figure 7: (a)–(c) The oscillating plots of τ_s, τ_m, τ_t, against R_i.

4.1. Nonoscillating/Steady Plots of Velocity U, Temperature θ, and Magnetic Distribution ϕ. 4.2. Oscillating Plots of Transient Shear-Stress τ_s, Heat Rate τ_t, and Current-Density τ_m. Figures 5(a)–5(c) depicted the transient and oscillating plots of shear stress τ_s, heat transfer τ_t, and current density τ_m against some favorable values of reduced gravity R_g in the presence of magnetohydrodynamics and porous material. It is shown that the amplitude of oscillations in terms of τ_s, τ_t for increasing values of reduced gravity parameter Rg is increased but on the other hand it is decreased for τ_m R_g. Because buoyant energies can induce the motion of fluid in the lower gravity within weak gravitational-fields and surface tension and density fluctuations may produce it in the presence of a gravitational field. The τ_s profile is increased for lower R_g but decreased at higher R_g due to porous material. Similarly, the τ_t profile depicted higher oscillating behavior for low gravity with good variations along the magnetized porous cone. Figures 6(a)–6(c) are drafted for some choices of porous parameter Ω to find oscillating and fluctuating current density, heat rate and shear stress along the magnetized heated cone. The increasing amplitude of fluctuation with prominent variations in current density and shear stress is deduced for every choice of Ω with Pr = 10.0. According to a physical point of view, this can be evident that when Pr rises, heat transmission with respect to thermal-diffusion reduces, and thickness of the fluid's velocity falls due to the retarding force the fluid must contend with while moving. The lower amplitude in the oscillations of heat rate is sketched for each choice of Ω but prominent variations are noted for each plot. The current density and shear stress are enhanced for lower Ω but decreased for higher Ω due to reduced gravity. In Figures 7(a)–7(c), the amplitude of current density is increased for each Richardson parameter R_i than other plots. The similar behavior in heat and shear stress with lower amplitude is drafted at every choice of R_i in magnetized porous cone because mixed convection acts similar to a pressure gradient for enhancing the fluid current density.

5. Conclusions

The current physical phenomena deals with the effects of reduced gravity on transient quantities of mixed convective rate of heat quantities along the magnetized heated cone immersed in porous material. For coupled form of partial differential equations subjected to the boundary conditions, the proposed unsteady nonlinear mathematical model is presented. The primitive variable formulation isused to transform the system of partial differential equations into primitiveform for smooth integration and to design the numerical algorithm. Later, large simulations are run using the implicit finite difference method for a range of parameter values. The reduced gravity parameter R_g, the Richardson parameter λ, the Prandtl number Pr, the porosity parameter Ω, and several other fixed parameters were all used to reach the numerical solutions of the coupled dimensionlized

equations. Plots are made for several governing parameters in the necessary modeled equations, including magnetic intensity, temperature and velocity profile, fluctuating shear tress graph, graph of heat rate, and graph of current density. Additionally, via careful examination and intentional discussion of physical reasoning, the physical impacts of various factors on the material qualities are examined. Following a numerical analysis of the process under consideration, the key findings are summarized as follows:

(i) In the cases of magnetic ϕ and temperature θ field plots, the greatest magnitude of the velocity distribution is obtained at $R_g = 1.5$, while it is obtained at $R_g = 0.1$ for the other cases.

(ii) Plots make it clear that while velocity value profiles are descending for decreasing values of Ω but magnetic ϕ and temperature θ field plots are ascending. The fact that the highest magnetic ϕ and temperature θ field plots are achieved for lower Ω is also noted.

(iii) The plots are deduced that ϕ and θ are decreased and u is increased for prominent choices of λ in the presence of Pr = 7.0. The prominent amplitude in velocity plots are deduced by increasing R_i because mixed convection impact.

(iv) It is shown that the amplitude of oscillationsin terms of τ_s, τ_t for increasing values of reduced gravity parameter Rg is increased but on theother hand it is decreased for τ_m R_g. Because buoyant energies can induce the motion of fluid in the lower gravity within weak gravitational-fields and surface tension and density fluctuations may produce it in the presence of a gravitational field.

(v) The lower amplitude in the oscillations of heat rate is sketched for each choice of Ω but prominent variations are noted for each plot.

(vi) The similar behavior in heat and shear stress with lower amplitude is drafted at every choice of λ in magnetized porous cone because mixed convection acts similar to a pressure gradient for enhancing the fluid current density.

(vii) This work can be extended for future work for the evaluation of heat transfer along the opaque surface of cone by including reduced gravity effects.

Nomenclature

T_∞: Ambient-temperature (K)
H_x, H_y: Magnetic field along xy-direction (Tesla)
u, v: Velocity along xy-direction (m s^{-1})
μ: Dynamic viscosity (kg m^{-1} s^{-1})
ν: Kinematic viscosity (m^2 s^{-1})
ρ: Density (kg m^{-3})
g: Gravitational-acceleration (m s^{-2})
β: Thermal-expansion (K^{-1})
ν_m: Magnetic-permeability (H m^{-1})
α: Thermal-diffusivity (m^2 s^{-1})
T: Fluid Temperature (K)
C_p: The specific-heat (J kg^{-1} K^{-1})
ϕ: Dimensionless magnetic field
k: Thermal conductivity
τ_s: Transient shear stress
MHD: Magnetohydrodynamic
τ_t: Transient heat transfer
H_o: Magnetic field intensity
τ_m: Transient current density
ρ_m: Maximum density
T_m: Temperature at maximum density
θ: Dimensionless temperature
R_g: Reduced gravity parameter
R_{e_L}: Reynolds number
γ: Magnetic Prandtl number
G_{r_L}: Grashof Number
ξ: Magnetic force parameter
U_∞: Free stream velocity
λ: Mixed convection parameter.

Data Availability

The data used in this study are available from the author upon request.

Conflicts of Interest

The authors declare that they have no conflicts of interest.

Authors' Contributions

All authors have worked equally. All authors have read and agreed to the published version of the manuscript.

Acknowledgments

The authors extend their appreciation to Prince Sattam bin Abdulaziz University for funding this research work through the project number PSAU/2023/01/21942.

References

[1] C. H. Chun and W. Wuest, "Experiments on the transition from the steady to the oscillatory Marangoni-convection of a floating zone under reduced gravity effect," *Acta Astronautica*, vol. 6, no. 9, pp. 1073–1082, 1979.

[2] J. M. Potter and N. Riley, "Free convection from a heated sphere at large Grashof number," *Journal of Fluid Mechanics*, vol. 100, no. 4, pp. 769–783, 1980.

[3] K. Anthony, H. K. Kuiken, and J. H. Merkin, "Boundary layer analysis of the thermal bar," *Journal of Fluid Mechanics*, vol. 303, pp. 253–278, 1995.

[4] A. J. Chamkha, "Magnetohydrodynamic mixed convection from a rotating cone embedded in a porous medium with heat generation," *Journal of Porous Media*, vol. 2, no. 1, pp. 87–105, 1999.

[5] A. J. Chamkha and A. R. Khaled, "Hydromagnetic simultaneous heat and mass transfer by mixed convection from a vertical plate embedded in a stratified porous medium with thermal dispersion effects," *Heat and Mass Transfer*, vol. 36, no. 1, pp. 63–70, 2000.

[6] K. A. Yih, "Radiation effect on mixed convection over an isothermal cone in porous media," *Heat and Mass Transfer*, vol. 37, no. 1, pp. 53–57, 2001.

[7] S. R. Mishra, G. C. Dash, and M. Acharya, "Mass and heat transfer effect on MHD flow of a visco-elastic fluid through porous medium with oscillatory suction and heat source," *International Journal of Heat and Mass Transfer*, vol. 57, no. 2, pp. 433–438, 2013.

[8] H. Dessie and N. Kishan, "MHD effects on heat transfer over stretching sheet embedded in porous medium with variable viscosity, viscous dissipation and heat source/sink," *Ain Shams Engineering Journal*, vol. 5, no. 3, pp. 967–977, 2014.

[9] M. M. M. Abdou, E. R. El-Zahar, and A. J. Chamkha, "MHD mixed convection stagnation- point flow of a viscoelastic fluid towards a stretching sheet in a porous medium with heat generation and radiation," *Canadian Journal of Physics*, vol. 93, no. 5, pp. 532–541, 2015.

[10] P. G. Metri, P. G. Metri, S. Abel, and S. Silvestrov, "Heat transfer in MHD mixed convection viscoelastic fluid flow over a stretching sheet embedded in a porous medium with viscous dissipation and non-uniform heat source/sink," *Procedia Engineering*, vol. 157, no. 40, pp. 309–316, 2016.

[11] M. Y. Malik, H. Jamil, T. Salahuddin, S. Bilal, K. U. Rehman, and Z. Mustafa, "Mixed convection dissipative viscous fluid flow over a rotating cone by way of variable viscosity and thermal conductivity," *Results in Physics*, vol. 6, pp. 1126–1135, 2016.

[12] P. Sudhagar, P. K. Kameswaran, and B. Rushi Kumar, "Magnetohydrodynamics mixed convection flow of a nanofluid in an isothermal vertical cone," *Journal of Heat Transfer*, vol. 139, no. 3, Article ID 34503, 2017.

[13] A. M. M. Raju, G. S. S. Raju, and B. Mallikarjun, "Unsteady quadratic convective flow of a rotating non-Newtonian fluid over a rotating cone in a porous medium," *International Journal of Advanced Research in Computer Science*, vol. 8, no. 6, 2017.

[14] M. A. Lotto, K. M. Johnson, C. W. Nie, and D. M. Klaus, "The impact of reduced gravity on free convective heat transfer from a finite, flat, vertical plate," *Microgravity Science and Technology*, vol. 29, no. 5, pp. 371–379, 2017.

[15] M. Ashraf, A. Fatima, and R. S. R. Gorla, "Periodic momentum and thermal boundary layer mixed convection flow around the surface of a sphere in the presence of viscous dissipation," *Canadian Journal of Physics*, vol. 95, no. 10, pp. 976–986, 2017.

[16] M. Ashraf and A. Fatima, "Numerical simulation of the effect of transient shear stress and rate of heat transfer around different positions of sphere in the presence of viscous dissipation," *Journal of Heat Transfer*, vol. 140, no. 6, Article ID 61701, 2018.

[17] J. Alhamid, A. R. Al-Obaidi, and H. Towsyfyan, "A numerical study to investigate the effect of turbulators on thermal flow and heat performance of a 3D pipe," *Heat Transfer*, vol. 51, no. 3, pp. 2458–2475, 2022.

[18] A. R. Al-Obaidi and J. Alhamid, "Investigation of flow pattern, thermohydraulic performance and heat transfer improvement in 3D corrugated circular pipe under varying structure configuration parameters with development different correlations," *International Communications in Heat and Mass Transfer*, vol. 126, Article ID 105394, 2021.

[19] A. R. Al-Obaidi and J. Alhamid, "Investigation of thermohydraulics flow and augmentation of heat transfer in the circular pipe by combined using corrugated tube with dimples and fitted with varying tape insert configurations," *International Journal of Heat and Technology*, vol. 39, no. 2, pp. 365–374, 2021.

[20] J. Alhamid and R. A. Al-Obaidi, "Flow pattern investigation and thermohydraulic performance enhancement in three-dimensional circular pipe under varying corrugation configurations," *Journal of Physics: Conference Series*, vol. 1845, no. 1, Article ID 12061, 2021.

[21] Z. Ullah, M. Ashraf, I. E. Sarris, and T. E. Karakasidis, "The impact of reduced gravity on oscillatory mixed convective heat transfer around a non-conducting heated circular cylinder," *Applied Sciences*, vol. 12, no. 10, p. 5081, 2022.

[22] G. Rasool, N. A. Shah, E. R. El-Zahar, and A. Wakif, "Numerical investigation of EMHD nanofluid flows over a convectively heated riga pattern positioned horizontally in a Darcy-Forchheimer porous medium: application of passive control strategy and generalized transferlaws," *Wavesin Randomand Complex Media*, pp. 1–20, 2022.

[23] A. Rauf, N. Ali Shah, A. Mushtaq, and T. Botmart, "Heat transport and magnetohydrodynamic hybrid micropolarferrofluid flow over a non-linearly stretching sheet," *AIMS Mathematics*, vol. 8, no. 1, pp. 164–193, 2023.

[24] T. Oreyeni, N. A. Shah, A. O. Popoola, E. R. Elzahar, and S. J. Yook, "The significance of exponential space-based heat generation and variable thermophysical properties on the dynamics of Casson fluid over a stratified surface with non-uniform thickness," *Waves in Random and Complex Media*, pp. 1–19, 2022.

[25] N. A. Shah, D. Vieru, and E. R. El-Zahar, "An analytical study of the unsteady nonlinear convection flow of nanofluids in an infinitely rectangular channel," *Waves in Random and Complex Media*, pp. 1–19, 2022.

[26] D. Vieru, C. Fetecau, N. A. Shah, and S. J. Yook, "Unsteady natural convection flow due to fractional thermal transport and symmetric heat source/sink," *Alexandria Engineering Journal*, vol. 64, pp. 761–770, 2023.

[27] M. J. Babu, Y. S. Rao, A. S. Kumar et al., "Squeezed flow of polyethylene glycol and water based hybrid nanofluid over a magnetized sensor surface: a statistical approach," *International Communications in Heat and Mass Transfer*, vol. 135, Article ID 106136, 2022.

[28] N. Zeeshan, N. A. Ahammad, H. U. Rasheed, A. A. El-Deeb, B. Almarri, and N. A. Shah, "A numerical intuition of activation energy in transient MicropolarNanofluid flow configured by an exponentially extended plat surface with thermal radiation effects," *Mathematics*, vol. 10, no. 21, p. 4046, 2022.

[29] A. Abderrahmane, N. A. Qasem, O. Younis et al., "MHD hybrid nanofluid mixed convection heat transfer and entropy generation in a 3-D triangular porous cavity with zigzag wall and rotating cylinder," *Mathematics*, vol. 10, no. 5, p. 769, 2022.

[30] H. B. Santhosh, M. S. Upadhya, N. A. Ahammad, C. S. K. Raju, N. A. Shah, and W. Weera, "Comparative analysis of a cone, wedge, and plate packed with microbes in non-fourier heat flux," *Mathematics*, vol. 10, no. 19, p. 3508, 2022.

[31] V. Nagendramma, P. Durgaprasad, N. Sivakumar et al., "Dynamics of triple diffusive free convective MHD fluid flow: lie group transformation," *Mathematics*, vol. 10, no. 14, p. 2456, 2022.

[32] F. Shahzad, W. Jamshed, T. Sajid et al., "Electromagnetic control and dynamics of generalized burgers' nanoliquid flow containing motile microorganisms with Cattaneo–Christov relations: galerkin finite element mechanism," *Applied Sciences*, vol. 12, no. 17, p. 8636, 2022.

[33] M. S. Ram, K. Spandana, M. Shamshuddin, and S. O. Salawu, "Mixed convective heat and mass transfer in magnetized micropolar fluid flow toward stagnation point on a porous stretching sheet with heat source/sink and variable species reaction," *International Journal of Modelling and Simulation*, pp. 1–13, 2022.

[34] S. O. Salawu, A. M. Obalalu, and M. D. Shamshuddin, "Nonlinear solar thermal radiation efficiency and energy optimization for magnetized hybrid Prandtl–Eyringnanoliquid in aircraft," *Arabian Journal for Science and Engineering*, vol. 48, no. 3, pp. 3061–3072, 2022.

[35] S. O. Salawu, H. A. Ogunseye, M. D. Shamshuddin, and A. B. Disu, "Reaction-diffusion of double exothermic couple stress fluid and thermal criticality with Reynold's viscosity and optical radiation," *Chemical Physics*, vol. 561, Article ID 111601, 2022.

[36] M. D. Shamshuddin, F. Mabood, G. R. Rajput, O. A. Bég, and I. A. Badruddin, "Thermo-solutal dual stratified convective magnetized fluid flow from an exponentially stretching Riga plate sensor surface with thermophoresis," *International Communications in Heat and Mass Transfer*, vol. 134, Article ID 105997, 2022.

[37] A. Abbas, M. Ashraf, Y. M. Chu, S. Zia, I. Khan, and K. S. Nisar, "Computational study of the coupled mechanism of thermophoretic transportation and mixed convection flow around the surface of a sphere," *Molecules*, vol. 25, no. 11, p. 2694, 2020.